INSTITUTE OF PHYSICS PUBLISHING NANOTECHNOLOGY
Nanotechnology **15** (2004) 1549–1553 PII: S0957-4484(04)82653-9

Europium-doped yttrium silicate nanoparticles embedded in a porous SiO_2 matrix

N Taghavinia[1,4], G Lerondel[2], H Makino[3] and T Yao[3]

[1] Physics Department, Sharif University of Technology, PO Box 11365-9161, Tehran 14588, Iran
[2] Laboratoire de Nanotechnologie et d'Instrumentation Optique, Université de Technologie de Troyes, 10010 Troyes cedex, France
[3] Institute for Materials Research, Tohoku University, Sendai 980-8577, Japan

E-mail: taghavinia@sharif.edu

Received 20 June 2004, in final form 19 August 2004
Published 1 October 2004
Online at stacks.iop.org/Nano/15/1549
doi:10.1088/0957-4484/15/11/031

Abstract
Europium-doped yttrium silicate nanoparticles were grown inside a porous silicon oxide matrix by chemical impregnation of porous silicon layers, followed by heat treatments. The average size of the nanoparticles is 50 nm and they are dispersed almost uniformly within the whole porous layer. Local composition measurements demonstrate that Y and Eu are found only in nanoparticles, indicating a good phase separation efficiency. There is indirect evidence that yttrium silicate nanoparticles are nucleated around Eu ions. The crystalline phase of the particles is pure α-$Y_2Si_2O_7$, with no trace of Y_2O_3 or Y_2SiO_5 or other $Y_2Si_2O_7$ polymorphs. Structural purity is an advantage for this method, as in the case of powder or sol–gel methods single-phase yttrium silicate formation is hardly possible, even at high firing temperatures.

1. Introduction

The synthesis of functional nanoparticles is still a challenge in the field of nanotechnology, and comprises a major body of research in this field. There are various methods developed to synthesize nanoparticles, either in a stand-alone form or inside a host matrix. Nanoparticles inside a matrix have the advantage that are stabilized, separated from each other by the matrix material and in some cases surface passivated. Nanoparticles in a matrix material form effectively a nanocomposite with properties inherited from both the matrix material and the nanoparticle guest material.

A common way to produce nanoparticles in a matrix host is to impregnate porous materials. The space inside porous materials allows introducing materials inside their body and forming nanoparticles in the free space inside. As a matrix, different porous materials have been tried. Zeolites are well-defined crystalline structures with an internal porous open framework of molecular dimensions. Various semiconductor nanocrystals have been grown into the pores of zeolites by ion-exchange reactions [1]. Porous silica, synthesized by the sol–gel method, has also been exploited as a host for nanocrystals, such as Ag [2], In_2O_3 [3] and CdSe [4]. Commercially available porous glass, which is obtained from acid leaching of heat-treated alkali–borosilicate glass, was also tried as a host for incorporated semiconductor nanocrystals, such as GaAs [5], InP [6] and ZnS:Cu [7]. Impregnation of porous silicon has also been achieved with different materials and in different methods. The incorporation of metals, in an attempt to attain electrical contacts to porous silicon, has been done mostly by electroplating [8] or simple immersion methods [9]. New luminescence structures with porous silicon have been reported by ion implantation, for example of Er [10], or solution impregnation, for example of dyes [11]. There are also reports on impregnation with semiconductor nanocrystals, such as CdSe [12].

We have recently developed a method to synthesize zinc silicate nanoparticles inside oxidized porous silicon and porous

[4] Author to whom any correspondence should be addressed.

glass [13–16]. Zinc silicate nanoparticles were doped with Mn^{2+} ions, and high Mn luminescence efficiency was achieved. The method is based on the insertion of Zn and Mn salts solutions into the pores of porous silicon and porous glass and subsequent thermal treatment. The porous SiO_2 host acts both as a medium to hold the finally formed nanoparticles, as well as one of the ingredients in the reactions to form the zinc silicate nanoparticles. This new idea can be applied to other silicate materials to form silicate nanoparticles in porous SiO_2.

In this work we demonstrate the growth of europium-doped yttrium silicate nanoparticles inside the pores of oxidized porous silicon and study the structural properties. Among the silicate materials zinc silicate and yttrium silicate are particularly important, as they are hosts for some important phosphor activators. Yttrium silicate if doped with Eu^{3+} emits strongly in red and if doped with Ce^{3+} is an efficient blue emitter. Y_2SiO_5:Eu^{3+}, Zn_2SiO_4:Mn^{2+} and Y_2SiO_5:Ce^{3+} are phosphors covering the whole range of the visible spectrum from red to blue. They are efficient phosphors for vacuum ultraviolet excitation, and are chemically stable. Hence, they are good choices as plasma display phosphors. These silicate phosphor nanoparticles, dispersed uniformly in a transparent porous layer of SiO_2, suggest an alternative for the conventional powder phosphor-based display technologies.

Y_2SiO_5-based powder phosphors are synthesized by solid-state reaction of Y_2O_3, SiO_2 and the activators at high temperature. If the reaction proceeds up to the thermodynamic equilibrium, the resulting phase would be a monoclinic phase, represented as X_2–Y_2SiO_5, with the composition of Y_2SiO_5. However, in practice the reaction does not proceed to the thermodynamic equilibrium state at temperatures below 1700 °C. This is due to the limited diffusion of both SiO_2 and Y_2O_3, which are high melting temperature materials. As a result, the reaction occurs inhomogeneously and other phases appear in the final product. Apart from the non-reacted Y_2O_3 and SiO_2, the major other phases observed are the various polymorphs of $Y_2Si_2O_7$.

To enhance the reaction speed, some flux materials, such as YF_3 or more efficiently BaF_2, are added to the starting powders. The role of the flux is to act as a carrier and improve the diffusion. This method helps to synthesize single-phase Y_2SiO_5 or $Y_2Si_2O_7$ phosphors at temperatures of about 1550 °C. This temperature is yet not a practically convenient temperature to achieve. Other suggestions to make the reaction faster basically involve preparing starting materials with more close contact between SiO_2 and Y_2O_3, for instance, preparation of reactive amorphous silicates containing stoichiometric amounts of the elements [17], or coating SiO_2 powder particles with Y_2O_3. These methods also require firing at temperatures as high as 1550 °C for the reaction to be completed.

More recently, Zhang *et al* have reported the synthesis of X_1–Y_2SiO_5:Eu using a sol–gel method [18–20]. The method involves creating a gel with stoichiometric composition that is then crushed into powder and fired. Temperatures as low as 900 °C could crystallize the X_1–Y_2SiO_5 phase; however, temperatures as high as 1500 °C are needed to have a single silicate phase without Y_2O_3 phase present [20]. The use of a porous gel structure improves the speed of the solid-state reaction, since it provides a high surface area for the ingredient reactions. This is the reason why this method is capable of the crystallization of a silicate phase at 900 °C. The reason for the remaining Y_2O_3 phase for firing temperatures below 1500 °C is probably the shortage of SiO_2 for the reaction. The problem might be relaxed by starting with an SiO_2-rich gel.

In this work we employ the idea of 'silicates in porous media' to synthesize europium-doped yttrium silicate in a transparent porous SiO_2 matrix at relatively low temperatures, and study the structural properties.

2. Experimental details

Porous silicon layers were formed on a p^+-type (100) Si wafer by the conventional electrochemical process. The average porosity and pore size were 70% and 10 nm, respectively. The thickness was about 15 μm. A chemical solution containing $Y(NO_3)_3$ and $Eu(NO_3)_3$ with Eu/Y ratio of 7% was diffused into the pores of porous silicon for several minutes. This was done by putting the samples in the solution or by putting a drop of solution on the sample. The diffusion continues until it fills the whole space of the pores.

The samples were then dried and put into an electrical furnace. The temperature was raised in a low ramp up to 500 °C in order to evaporate water, dehydrate the nitrate molecules and dissociate them into the corresponding oxides. Then the temperature was increased to 1100–1250 °C and the samples were fired for several hours in air. The skeleton of porous silicon oxidizes completely soon after the temperature reaches about 900 °C. At the firing temperature the reaction of Y_2O_3, SiO_2 and Eu_2O_3 takes place and Eu-doped yttrium silicate phase in a porous SiO_2 matrix is formed. Hereafter we call this system PS:YS:Eu, PS and YS representing porous silicon and yttrium silicate, respectively. The uniformity of impregnation was examined by electron probe microanalysis (EPMA) images from a cross section of the samples. Figure 1 shows an SEM picture as well as the elemental composition images by EPMA. The sample was cut into two pieces and glued together face to face. A slice of the double sample was cut and polished on both sides for the observation. The black line in the centre in the SEM picture is the glue, and the two layers on both sides are PS:YS:Eu layers. The outer parts are the silicon substrates. EPMA images show that Y is found almost uniformly all over the layer, indicating that the whole layer has been effectively impregnated. As expected, Si is found both in the substrate and in the layer and O is only found in the layer.

3. Results and discussion

Figure 2(a) shows a cross section transmission electron microscope (TEM) image at the bottom of the PS:YS:Eu layer. The black particles are yttrium silicate phase and the lighter areas are either SiO_2 skeleton or the pores. There is a distribution of size, with average particle size of about 50 nm. A uniform SiO_2 layer has been grown at the bottom by thermal oxidation of the silicon substrate during the firing. The thickness of the layer is about 500 nm. The interface between the SiO_2 layer and porous layer is the front of the PS growth, and is seen to be relatively rough. The roughness partly comes from the anisotropic growth of pores in the direction normal to the wafer surface. A parallel pore structure can be clearly seen

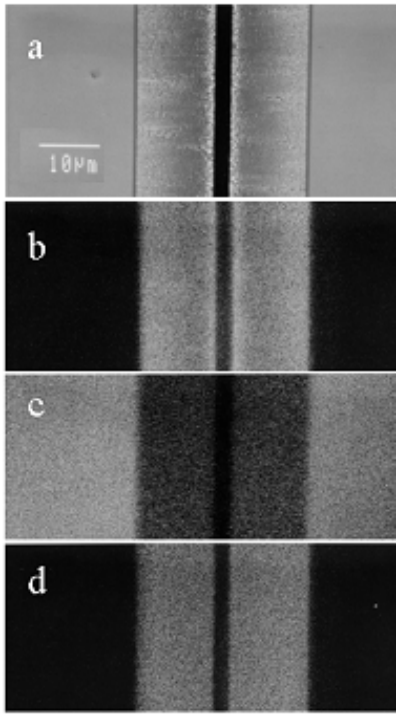

Figure 1. (a) SEM picture of a cross section of a PS:YS:Eu sample. Two similar samples are attached to each other face to face using a glue layer. ((b), (c), (d)) EPMA images showing the concentrations of Y, Si and O, respectively. Darker areas denote higher concentrations.

in the figure. This is a feature of meso-porous silicon grown on p^+-type wafers.

The pore structure and size are more apparently seen in the plan view TEM (figure 2(b)). The white spots are the cross section of parallel, pipe-like pores. The average pore diameter is about 30 nm, which is considerably larger than the pore diameter of the starting porous silicon (10 nm). This enlargement has been attributed to the restructuring of the pores after or during oxidation, in order to reduce the surface energy [15]. Figure 2(c) shows the spectra taken by energy dispersive x-ray spectroscopy (EDS) from points A and B, marked on the TEM image. In point B the only elements present are Si and O, while in point A there are also Y and Eu. This demonstrates that the dark spots are YS particles doped with Eu. Lack of Y and Eu in other parts indicates that the impregnating species are not dissolved in SiO_2, forming a glass phase, but rather have segregated into a silicate phase.

Quantitative measurements indicate that the average Eu/Y ratio inside the silicate particles is 10%, compared with 7% in the starting solution. In other words, the Eu concentration in the formed silicate particles is more than that of the solution stoichiometry. This might be evidence that the Eu species provide nucleation centres for the formation of the yttrium silicate phase. This provides a means for effective doping of the nanoparticles formed in the porous matrix. For Zn_2SiO_4:Mn in oxidized porous silicon it was shown that there is a self-controlled doping mechanism for Mn ions, which leads to efficient doping of Zn_2SiO_4. It originates from the very low tendency of MnO_x to react with SiO_2, in contrast to the fast reaction with Zn_2SiO_4. In the case of YS:Eu, it seems that

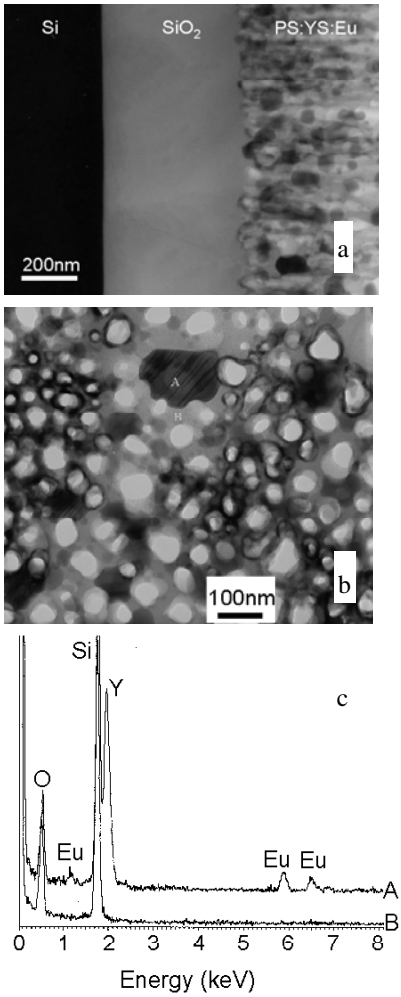

Figure 2. (a) Cross section TEM image of the bottom of the porous PS:YS:Eu layer. (b) Top view TEM image of the PS:YS:Eu layer. (c) EDS spectra of points A (black area) and B (grey area).

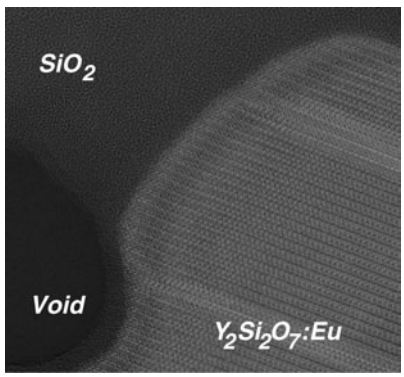

Figure 3. TEM image of the area containing crystalline YS, amorphous SiO_2 and the void. The picture is a negative image.

a different mechanism is involved that enhances the doping efficiency, and it originates from the fact that the Eu species provide nucleation centres for YS phase formation.

The high resolution TEM image demonstrates that the particles are not amorphous, but crystalline. Figure 3 shows an area where the crystalline YS and amorphous SiO_2 and the void in the porous structure meet. It is turned into a negative image

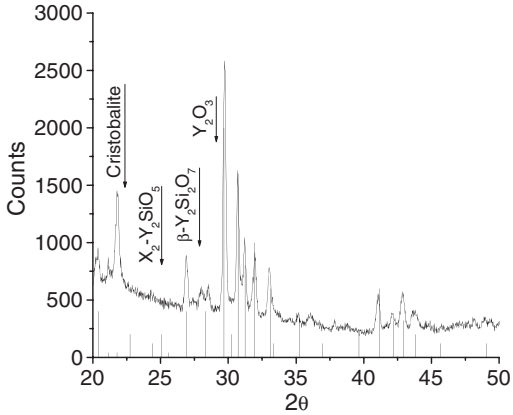

Figure 4. XRD pattern for a PS:YS:Eu sample. The vertical lines show the peak positions and intensity for α-$Y_2Si_2O_7$ phase. The arrows show the position of a strong peak of the indicated phase.

for a better view. There are dislocation lines in the crystal that might be due to stacking faults.

The x-ray diffraction (XRD) pattern of a sample fired at 1250 °C is displayed in figure 4. The XRD pattern for samples fired at 1100 °C is essentially the same. The positions of the peaks are in good correspondence with the peaks of α-$Y_2Si_2O_7$ phase, as reported by Ito and Johnson [17]. The position and intensity of peaks in their report is included in the figure. In the reported work, α-$Y_2Si_2O_7$ was synthesized by fusion at 1190 °C. The report however does not include all the peaks, and the indexing of peaks cannot be done in a very precise way. Nevertheless, a triclinic phase with $a = 6.59$ Å, $b = 6.64$ Å, $c = 12.25$ Å, $\alpha = 94.0°$, $\beta = 89.2°$, $\gamma = 93.1°$ can index most of the peaks. The XRD for our sample is slightly different from the reported one in the position of peaks, the relative intensities and disappearance of a few peaks. The slight difference in peak positions can be attributed to the difference in composition, as in our case α-$Y_2Si_2O_7$ is doped with Eu. Most of the peaks in our sample are slightly shifted to lower angles, implying slightly larger lattice constants. This is expected, as the ionic radius of Eu^{3+} is 0.95 Å compared to 0.89 Å for Y^{3+}.

The existence of Eu can also affect the relative intensity of peaks. It has been shown that doping affects the structure factor in certain directions, in particular if the doping atom occupies an interstitial position [21]. Modulation of structure factor changes the relative peak intensities. The difference in relative peak intensities can also be due to the anisotropic distribution of α-$Y_2Si_2O_7$ crystalline particles in the porous matrix, i.e. the particles being grown in some preferred crystallographic directions. In any case, the agreement between the two data is sufficient to conclude that the phase of the crystalline particles is α-$Y_2Si_2O_7$.

As mentioned earlier, the formation of the silicates of yttrium using conventional methods usually leads to incomplete reaction, leaving unreacted Y_2O_3 and SiO_2, and the occurrence of multiple silicate phases. Single-phase products are only possible by using flux materials and firing at 1550 °C. Even with the sol–gel method it has not been possible to synthesize single-phase material by firing below 1500 °C [20]. However, we find that the formation of a single-phase yttrium silicate is possible by synthesizing it in a porous SiO_2 matrix. The positions of one of the strong peaks of some possible phases are shown in figure 4. There is apparently no trace of Y_2O_3, indicating that all the oxide is consumed in the reaction. This is in part due to the SiO_2-rich condition in the porous SiO_2. On the other hand, the nanometre size mixing of the two phases of Y_2O_3 and SiO_2 causes their reaction fully occur at temperatures as low as 1100 °C. As the initial size of Y_2O_3 grains and the SiO_2 skeleton is about 10 nm, it is possible that the low size reduces the melting temperature, hence enhancing their diffusion into each other.

Other phases of yttrium silicate also were not observed. Apart from the low temperature y-yttrium silicate that occurs in certain conditions, yttrium silicate is found mainly in two stoichiometries: Y_2SiO_5 and $Y_2Si_2O_7$ [22]. X_1–Y_2SiO_5 and X_2–Y_2SiO_5 are the two polymorphs of Y_2SiO_5 which occur below and above 1190 °C. α-, β-, γ- and δ- are the known polymorphs of $Y_2Si_2O_7$, which transform from one to another with increasing temperature. The sequence of transformation is [17]:

$$\alpha \xleftrightarrow{1225\,^\circ\mathrm{C}} \beta \xleftrightarrow{1445\,^\circ\mathrm{C}} \gamma \xleftrightarrow{1535\,^\circ\mathrm{C}} \delta. \qquad (1)$$

The reason that Y_2SiO_5 phases have not appeared can be explained by the SiO_2-rich conditions in the porous samples. β-$Y_2Si_2O_7$ has not occurred in the porous samples, even at 1250 °C firing temperature. The transformation temperature between α- and β-phase was reported as 1225 °C in $Y_2Si_2O_7$ [17]. The occurrence of α-phase even at 1250 °C can be due to Eu doping. α- to δ-phases exist also for other rare earth disilicates; however, the transformation temperature is different. The larger ionic radius of the rare earths stabilizes the α-phase up to higher temperatures [17]. As the Eu^{3+} radius is 0.95 compared to 0.89 for Y^{3+}, one expects that the transformation temperature of α- to β-phase is shifted to higher temperatures.

4. Conclusion

We have demonstrated the growth of Eu-doped yttrium silicate nanoparticles in oxidized porous silicon layers at relatively low temperature. EPMA images from the cross section of the layers show good uniformity of impregnation in depth. There is a relatively large nanoparticle size distribution, with an average size of about 50 nm. The particles are crystalline according to XRD spectra and TEM images. The crystalline phase of the nanoparticles is α-$Y_2Si_2O_7$ with no trace of Y_2O_3, Y_2SiO_5 and other polymorphs of $Y_2Si_2O_7$. The formation of a pure silicate phase at temperatures as low as 1100 °C distinguishes this method from powder or sol–gel methods in which 1500 °C firing is required to achieve single-phase products. EDS measurements indicate that the Eu concentration in the nanoparticles is higher than the Eu concentration in the starting impregnating solution. This is indirect evidence that yttrium silicate nanoparticles nucleate around Eu ions. This mechanism is probably the reason for the efficient incorporation of Eu impurity ions in yttrium silicate nanoparticles. Eu-doped yttrium silicate is an efficient phosphor and the PS:YS:Eu system could be a candidate for display applications. The luminescence properties of this material system will be published elsewhere.

Acknowledgments

The authors would like to thank the Laboratory for Advanced Materials of Institute for Materials Research, Tohoku university for the XRD, TEM and EPMA experiments.

References

[1] For example: Wang Y and Herron N 1987 *J. Chem. Phys.* **91** 257
[2] Weiping C and Lide Z 1997 *J. Phys.: Condens. Matter* **9** 7257
[3] Zhou H, Cai W and Zhang L 1999 *Mater. Res. Bull.* **34** 845
[4] Coffer J L, Beauchamp G and Zerda T W 1992 *J. Non-cryst. Solids* **142** 208
[5] Justus B L, Tonucciand R J and Berry A D 1992 *Appl. Phys. Lett.* **61** 3151
[6] Hendershot D G, Gaskill D K, Justus B L, Fatemi M and Berry A D 1993 *Appl. Phys. Lett.* **63** 3324
[7] Huston A L, Justus B L and Johnson T L 1996 *Appl. Phys. Lett.* **68** 3377
[8] Herino R, Jan P and Bomchil G 1985 *J. Electrochem. Soc.* **132** 2513
[9] Andsager D, Hillard J, Hetrick J M, Abuhassan L H, Plisch M and Nayfeh M H 1993 *J. Appl. Phys.* **74** 4783
[10] Namavar F, Lu F, Perry C H, Cremins A, Kalkhoran M N and Soref R A 1995 *J. Appl. Phys.* **77** 4813
[11] Li P, Li Q, Ma Y and Fang R 1996 *J. Appl. Phys.* **80** 490
[12] Belogorokhov A I, Belegorokhova L I, Perez-Rodriguez A, Morante R and Gavrilov S 1998 *Appl. Phys. Lett.* **73** 2766
[13] Taghavinia N, Lerondel G, Makino H, Parisini A, Yamamoto A, Yao T, Kawazoe Y and Goto T 2002 *J. Lumin.* **96** 171
[14] Taghavinia N, Lerondel G, Makino H, Yamamoto A, Yao T, Kawazoe Y and Goto T 2002 *J. Cryst. Growth* **237–239** 869
[15] Taghavinia N, Lerondel G, Makino H, Parisini A, Yamamoto A, Yao T, Kawazoe Y and Goto T 2002 *J. Electrochem. Soc.* **149** G251
[16] Taghavinia N, Lerondel G, Makino H, Yamamoto A, Yao T, Kawazoe Y and Goto T 2001 *Nanotechnology* **12** 547
[17] Ito J and Johnson H 1968 *Am. Mineral.* **53** 1940
[18] Zhang W, Xie P, Duan C, Yan K, Yin M, Lou L, Xia S and Krupa J C 1998 *Chem. Phys. Lett.* **292** 133
[19] Yin M, Zhang W, Xia S and Krupa J C 1996 *J. Lumin.* **68** 335
[20] Yin M, Duan C, Zhang W, Lou L, Xia S and Krupa J C 1999 *J. Appl. Phys.* **86** 3751
[21] Goyal D J, Agashe C, Marathe B R, Takwale M G and Bhide V G 1993 *J. Appl. Phys.* **73** 7520
[22] Liddell K and Thomson D P 1986 *Ceram. Trans. J.* **85** 17